Available online at www.sciencedirect.com
SCIENCE DIRECT®
Transportation Research Part C 12 (2004) 369–400
TRANSPORTATION RESEARCH PART C
www.elsevier.com/locate/trc

# Recognition and tracking of spatial–temporal congested traffic patterns on freeways

Boris S. Kerner *, Hubert Rehborn, Mario Aleksic, Andreas Haug

*Daimler Chrysler AG, Telematics Research (RIC/TS), HPC: T729, D-73734 Esslingen, Germany*

Received 9 July 2001; received in revised form 2 April 2003

**Abstract**

The two models FOTO (Forecasting of Traffic Objects) and ASDA (Automatische Staudynamikanalyse: Automatic Tracking of Moving Traffic Jams) for the automatic recognition and tracking of congested spatial–temporal traffic flow patterns on freeways are presented. The models are based on a *spatial–temporal* traffic phase classification made in the three-phase traffic theory by Kerner. In this traffic theory, in congested traffic two different phases are distinguished: ''wide moving jam'' and ''synchronized flow''. The model FOTO is devoted to the identification of traffic phases and to the tracking of synchronized flow. The model ASDA is devoted to the tracking of the propagation of moving jams. The general approach and the different extensions of the models FOTO and ASDA are explained in detail. It is stressed that the models FOTO and ASDA perform without any validation of model parameters in different environmental and traffic conditions. Results of the online application of the models FOTO and ASDA at the TCC (Traffic Control Center) of Hessen near Frankfurt (Germany) are presented and evaluated.


*Keywords:* Local traffic measurements on freeways; Classification of traffic phases; Tracking of spatial–temporal congested patterns; Freeway bottlenecks; Suitability of the freeway infrastructure for congested pattern recognition; Traffic control center; Field trial evaluation of models ASDA/FOTO; Three-phase traffic theory; Wide moving jams; Synchronized traffic flow

* Corresponding author.
*E-mail address:* boris.kerner@daimlerchrysler.com (B.S. Kerner).

0968-090X/$ - see front matter © 2004 Elsevier Ltd. All rights reserved.
doi:10.1016/j.trc.2004.07.015

## 1. Introduction: Spatial–temporal pattern classification

It is well-known that traffic on freeways can be either, ''free'' or ''congested''. The congested regime of traffic shows very complex spatial–temporal traffic patterns (e.g., the classical works by Treiterer, 1975; Koshi et al., 1983). Therefore, the online automatic recognition and tracking of traffic patterns in the congested regime is one of the main problems for traffic control centers where measurements of traffic flow are collected and interpreted.

One of the approaches and trials in traffic technology to estimate, track and predict traffic patterns is an application of either microscopic (in particular, the car-following models), mesoscopic or macroscopic traffic flow models which calculate the movement of individual vehicles and/or the average vehicle speed and the density spatial–temporal distributions in freeway networks (e.g., Wiedemann, 1974; Cremer, 1979; May and Keller, 1968; Papageorgiou, 1983; Ben-Akiva et al., 1994; Daganzo, 1994; Gartner et al., 1997; Kronjäger and Konhäuser, 1997; Kates and Bogenberger, 1997; Leutzbach, 1988; Kaumann et al., 2000; review of traffic models by Helbing, 2001). Traffic data measured at some locations on a freeway can be used as some kind of ''boundary conditions'' for these mathematical traffic flow models which should calculate spatial–temporal distributions of traffic variables on the whole freeway. Unfortunately, practical online applications of this approach have some principle problems. One of the main problems is the necessity of a validation of some model parameters. These parameters are strongly dependent on the infrastructure, the weather and other environmental conditions. Therefore, it is very hard to find and adapt a set of the model parameters which are valid for real traffic flow in all possible totally different conditions. This is one of the principle reasons why the mentioned models are up to now far from being used for practical online applications on freeways. Another principal problem for online application of this model approach is associated with the probabilistic nature of conjested patterns at bottlenecks: Depending on initial conditions different types of the patterns can occur at the same traffic demand and traffic conditions.

Recently Kerner, in collaboration with Rehborn, has found out that two qualitatively different traffic phases should be distinguished in the congested regime of traffic: ''synchronized traffic flow'' and ''wide moving traffic jams'' (Kerner and Rehborn, 1996a). Therefore, there are three traffic phases: (i) free traffic flow, (ii) synchronized traffic flow and (iii) wide moving traffic jams. Based on these empirical findings, Kerner developed a three-phase traffic theory, which allows to explain results of empirical observations of the phase transitions between these three traffic phases and the spatial–temporal properties of patterns in congested traffic at freeway bottlenecks (Kerner, 1998a,b; Kerner, 1999a,b,c; Kerner, 2000a,b,c; Kerner, 2001a,b; Kerner, 2002a,b,c; Kerner, 2004a). Based on this theory, Kerner proposed a model approach to the spatial–temporal congested traffic pattern recognition, tracking and prognosis on freeways which has been realized in the models ASDA (Kerner et al., 1998; Kerner and Rehborn, 2000) and FOTO (Kerner et al., 2001a; Kerner, 2001b).

Note that a detailed consideration of empirical congested traffic pattern features on German, American, and Canadian freeways, the physics and theory of the onset of congestion and congested traffic patterns, engineering applications of the physics of traffic (congested pattern recognition, tracking, prediction, and control) is recently made in the book (Kerner, 2004b).

The model FOTO (Forecasting of Traffic Objects) identifies the traffic phases and performs the tracking of the patterns of the traffic phase ''synchronized flow''. The model ASDA

(Automatische Staudynamikanalyse: Automatic Tracking of Moving Traffic Jams) performs the automatic tracking of the propagation of moving traffic jams.

It must be noted that in contrast to the conventional model approach mentioned above, the models FOTO and ASDA perform without *any validation of model parameters* in different environmental and traffic conditions (see results in Kerner et al., 2000a,b,c; Kerner et al., 2001b,c; Kniss, 2000). Recall that according to the three-phase traffic theory a wide moving jam is a localized congested pattern which is spatially restricted by two upstream moving fronts where the average vehicle speed and the density sharply change. The both fronts of the wide moving jam propagate *continuously* upstream. Inside the wide moving jam each vehicle is in a stop at least for a finite time which is large enough that there is no influence of the traffic upstream of the wide moving jam on the traffic downstream and vice versa. Synchronized traffic flow is also separated spatially either from free flow or from a wide moving jam by the downstream front and by the upstream front where vehicle speed sharply changes. However, the flow rate in contrast to a wide moving jam can remain in synchronized flow almost constant inside these fronts.

To distinguish between wide moving jams and synchronized flow in the congested regime of traffic the following objective criteria can be applied (Kerner, 2000b,c). After a wide moving jam has emerged, it propagates through either free flow or any states of synchronized flow or any kinds of bottlenecks (e.g., on- and off ramps) *keeping* the velocity of the jam's downstream front. In contrast to a wide moving jam, after synchronized flow has occurred at a bottleneck the downstream front of the pattern of synchronized flow is usually fixed at the bottleneck. A more detailed consideration of empirical spatial–temporal features of synchronized flow and wide moving jams can be found in (Kerner, 2002b,c).

The main features of the approach FOTO and ASDA are the following (Kerner et al., 1998; Kerner and Rehborn, 2000; Kerner et al., 2001a; Kerner, 2001b): In FOTO based on local measurements of traffic (detectors D1 and D2 in Fig. 1) the local recognition of the traffic phases is

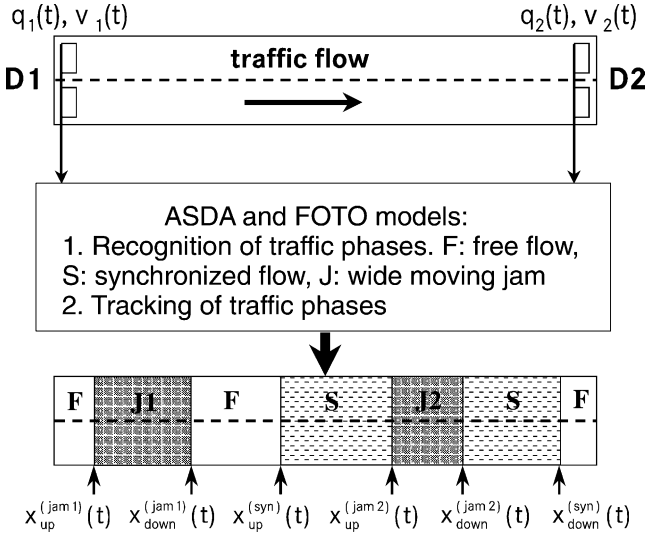


Fig. 1. Illustration of the approach of the models FOTO and ASDA (Kerner et al., 2001b).

performed first. Secondly, FOTO and ASDA perform the recognition of the moving fronts of wide moving jams $x_{up}^{(jam)}$, $x_{down}^{(jam)}$ and of the fronts of synchronized flow $x_{up}^{(syn)}$, $x_{down}^{(syn)}$ at the detectors. These fronts define the spatial size and location of the related "synchronized flow" object and "wide moving jam" object. Finally, the models FOTO and ASDA perform the tracking of these objects' fronts in time and space, i.e., the positions of all fronts $x_{up}^{(jam)}(t)$, $x_{down}^{(jam)}(t)$, $x_{up}^{(syn)}(t)$, $x_{down}^{(syn)}(t)$ as functions of time are found *between the detectors* where no measurements of traffic variables are possible. This tracking which is independent on the local measurements is related to the actual online description of the spatial–temporal features of the traffic objects.

In other words, in the approach FOTO and ASDA after the recognition of the traffic objects "synchronized flow" and "wide moving jam" at the detector locations these objects are tracked as *macroscopic single objects*, i.e., only the determination of the location of the object fronts and the object widths (in the longitudinal direction) *at any time* is the aim of the approach. This tracking of the traffic objects "synchronized flow" and "wide moving jam" performs also *between detectors*, i.e., also when the object fronts and the object widths cannot be measured at all. Note, that the models FOTO and ASDA allow us to predict a merging and/or a dissolution of initially different two or more traffic objects "synchronized flow" and of initially different two or more traffic objects "wide moving jam" which occur between locations of the detectors (a merging of wide moving jams with synchronized flow is not possible; see the objective criteria for the traffic phases above). Using the average vehicle speed and density within the traffic objects (which are known from empirical studies and current traffic measurements) one can calculate other traffic characteristics, e.g., trip travel times and/or vehicle trajectories.

In the article, the models FOTO and ASDA are formulated in detail. A statistical evaluation of FOTO and ASDA model results is made based on a four months field trial on freeways in the federal state "Hessen" (Germany). Based on empirical data the quality of the congested spatial–temporal pattern recognition and tracking under different detector configurations is studied. The article is organized as follows: A description of the model FOTO for the traffic phase recognition will be considered in Section 2. The tracking of wide moving jams with the model ASDA will be presented in Section 3. A tracking of synchronized flow will be discussed in Section 4. Results of the model application and evaluation will be presented in Section 5.

## 2. Determination of traffic phases with the model FOTO

The recognition of congested patterns with the model FOTO (Kerner et al., 2001a; Kerner, 2001b) will be limited here to traffic data measured at stationary detectors on freeways. In a practical application, for the classification of the traffic phases based on such local measurements a fuzzy inference system is used.

### 2.1. Set of fuzzy rules for traffic phase determination with FOTO

The current traffic measurements for each detector $q(t)$ and $v(t)$ are considered in a set of fuzzy rules. The fact that the flow rate in synchronized flow is usually much higher than the flow rate in wide moving traffic jams is taken into account as well as other empirical features of the traffic phases "synchronized flow" and "wide moving jam".

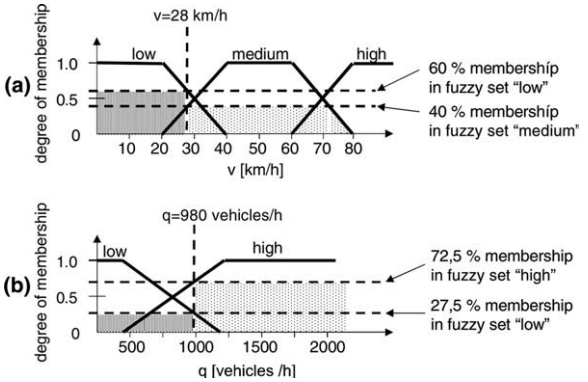


Fig. 2. Illustration of FOTO. Fuzzification of the input variables with the basic rules: (a) ''vehicle speed'' and (b) ''flow rate''. The degree of membership is determined for each fuzzy set by the membership function (see curves ''low'', ''medium'' and ''high'' in (a) and ''low'' and ''high'' in (b)). Dashed lines show the degrees of membership for an example with $v = 28$ km/h, $q = 980$ veh./h.

With the current flow rate fuzzified into the values ''low'' and ''high'' and the vehicle speed fuzzified into the values ''low'', ''medium'' and ''high'', the following fuzzy rules are implemented (Fig. 2):

**Rule1:** If the vehicle speed is ''high'', the traffic phase is ''free flow''.
**Rule2:** If the vehicle speed is ''medium'', the traffic phase is ''synchronized flow''.
**Rule3:** If the vehicle speed is ''low'' and the flow rate is ''high'', the traffic phase is ''synchronized flow''.
**Rule4:** If both the vehicle speed and the flow rate are ''low'', the traffic phase is ''wide moving jam''.

The numerical values of the membership functions are found based on the empirical data at the A5. It turns out that the same values may be used for all detectors at the A5-North and A5-South and for the rest of the Hessen freeways as well as for freeways near Magdeburg and Munich (Section 5.2). It may be expected that these numerical values can be influenced by traffic regulations (overtaking laws, variable speed limits, etc.) and peculiarities of the infrastructure (roadworks, narrow lanes, road gradient, etc.). Therefore, the numerical values have to be adapted for example for US freeways or inner-urban expressways with fixed speed limits. Additionally, an accident or a sudden road blockage can lead to the necessity of adapted membership functions because the infrastructure changes.

### 2.2. Defuzzification

Note, that the traffic phases recognized by the fuzzy rules are not numerical values. These phases are also not scalable among each other: For example, the traffic phase ''free flow'' cannot be weighted numerically in comparison with the traffic phase ''wide moving jam''. Therefore, the defuzzification is not performed with the standard methods COG (center of gravity) or MOM

(mean of maxima). Instead, the traffic state with the highest degree of membership after processing all fuzzy rules is used.

Let us demonstrate the use of these fuzzy sets for one example shown in Fig. 3. Table 1 related to Fig. 3 shows the degree of membership for the measured values of vehicle speed and flow rate, the degrees of membership for the four fuzzy rules and the classified traffic state at the detector D5 for some time moments between 8:45 and 9:10 am. The values for flow rates (“$q$” in veh./h and per lane) and vehicle speed (“$v$” in km/h) are fuzzified according to the fuzzy membership functions in Fig. 2. The membership values for flow rates (“low” and “high”) and speeds (“low”, “medium” and “high”) are in each minute used in the four fuzzy rules. The resulting traffic phase with the maximum degree of membership of the four fuzzy rules “Rule1–Rule4” can be found in the most

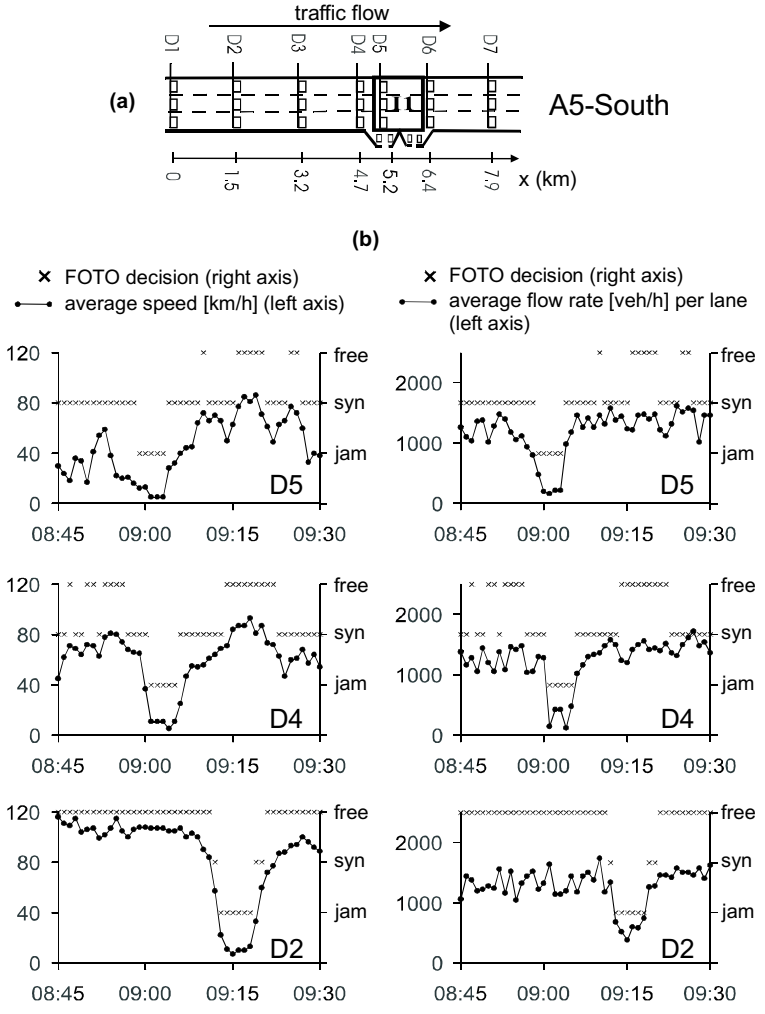


Fig. 3. Traffic phases determination with FOTO: (a) a part of the section of the freeway A5-South and (b) average speed (left) and flow rate (right) at detectors D5, D4 and D2 on 11th March, 2002 (left axis in each diagram) together with the corresponding decision of FOTO about the current traffic phase (right axis in each diagram).

Table 1
Example for the use of the four fuzzy rules in the model FOTO

| Time | $q$ | $v$ | Flow | | Speed | | | Rule1 | Rule2 | Rule3 | Rule4 | Phase |
|---|---|---|---|---|---|---|---|---|---|---|---|---|
| | | | Low | High | Low | Medium | High | "Free" | "Syn" | "Syn" | "Jam" | |
| 08:45 | 1260 | 30 | 0 | 1 | 0.5 | 0.5 | 0 | 0 | 0.5 | 0.5 | 0 | Syn |
| 08:46 | 1100 | 24 | 0.125 | 0.875 | 0.8 | 0.2 | 0 | 0 | 0.2 | 0.8 | 0.125 | Syn |
| …. | | | | | | | | | | | | |
| 08:57 | 940 | 21 | 0.325 | 0.675 | 0.95 | 0.05 | 0 | 0 | 0.05 | 0.675 | 0.325 | Syn |
| 08:58 | 800 | 16 | 0.5 | 0.5 | 1 | 0 | 0 | 0 | 0 | 0.5 | 0.5 | Syn |
| 08:59 | 480 | 12 | 0.9 | 0.1 | 1 | 0 | 0 | 0 | 0 | 0.1 | 0.9 | Jam |
| …. | | | | | | | | | | | | |
| 09:03 | 220 | 5 | 1 | 0 | 1 | 0 | 0 | 0 | 0 | 0 | 1 | Jam |
| 09:04 | 980 | 28 | 0.275 | 0.725 | 0.6 | 0.4 | 0 | 0 | 0.4 | 0.6 | 0.275 | Syn |
| …. | | | | | | | | | | | | |
| 09:09 | 1260 | 64 | 0 | 1 | 0 | 0.8 | 0.2 | 0.2 | 0.8 | 0 | 0 | Syn |
| 09:10 | 1460 | 72 | 0 | 1 | 0 | 0.4 | 0.6 | 0.6 | 0.4 | 0 | 0 | Free |

right column ("syn": synchronized flow, "jam": wide moving jam, "free": free traffic flow). The evaluation of this application will be made in Section 5. Note, that low speeds are measured at the detector D5 between 8:45 and 8:58 am. Despite these jam-like low speeds, the traffic state is classified as "synchronized flow" because the flow rate is still high.

However, in some cases the distinction between synchronized flow and wide moving jams based on the four fuzzy rules mentioned above is not accurate. To cope with such special measurement constellations, an extended set of fuzzy rules has been developed. The approach and an empirical example for the utility of the extended rules can be found in Appendix A.

## 3. Tracking of moving jams with the model ASDA

The model ASDA (Kerner et al., 1998; Kerner and Rehborn, 2000) is used to track a moving jam at all times, i.e., even when the moving jam is between detectors and therefore the jam cannot be measured. To get an overview on the model ASDA, let us consider Fig. 4 where in a schematic illustration the dynamic movement of a wide moving jam is shown on a freeway section at different times.

The schematic illustration for the model ASDA (Fig. 4(a)) shows a measurement infrastructure with two detectors ($Q_0, Q_n$) on a road section. After a moving jam has been observed in the cyclic measured data at $Q_n$ at time $t_0$ by the model FOTO, the model ASDA starts to calculate continuously the positions of the upstream front, $x_{\mathrm{up}}^{(\mathrm{jam})}(t)$. After the downstream front of the moving jam is registered at the detector $Q_n$ at the later time $t_1$, the model ASDA starts to calculate continuously the positions of the downstream front, $x_{\mathrm{down}}^{(\mathrm{jam})}(t)$ and consequently the jam width $L_S = x_{\mathrm{down}}^{(\mathrm{jam})} - x_{\mathrm{up}}^{(\mathrm{jam})}$. This can be done cyclically even if none of the detectors is within or close to the wide moving jam. For this calculation the measured traffic data of the vehicle flow rate $q_0(t)$ and $q_n(t)$ and the vehicle speeds $w_0(t)$ and $w_n(t)$ at the detectors $Q_0$ and $Q_n$ are needed. The model ASDA for this simple case has been published in (Kerner et al., 2001b).

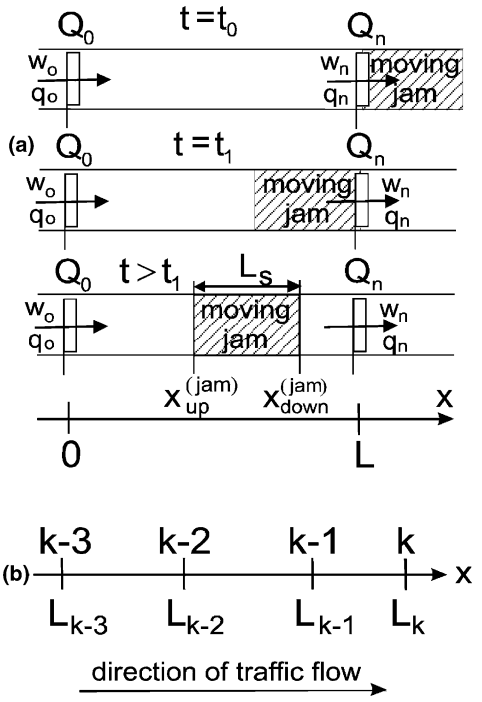


Fig. 4. Illustration of ASDA: (a) schema of the moving jam recognition with two detectors and (b) schema of a freeway section with several detectors with co-ordinates $L_{k-3},\ldots,L_k$.

### 3.1. Formulation of the model ASDA

In real applications several detectors following one another exist on freeways (Fig. 4(b)). In such a case the determination of the positions of the upstream and downstream front of a wide moving jam results in the following formula (1) and (2), respectively:

(a) Equation for the position of the upstream front of the moving traffic jam:

$$\begin{aligned} x_{\mathrm{up}}^{(\mathrm{jam})}(t) &= L_{i+1} + \int_{t_0^{(i+1)}}^{t} v_{\mathrm{up}}^{(\mathrm{jam})}(t)\,\mathrm{d}t \\ &\approx L_{i+1} - \int_{t_0^{(i+1)}}^{t} \frac{q_0^{(i)}(t) - q_{\min}}{\rho_{\max} - \left(q_0^{(i)}(t)/w_0^{(i)}(t)\right)}\,\mathrm{d}t, \quad t \geqslant t_0^{(i+1)}, \quad i = 1,2,\ldots \end{aligned} \tag{1}$$

(b) Equation for the position of the downstream front of the moving traffic jam:

$$x_{\mathrm{down}}^{(\mathrm{jam})}(t) = L_j + \int_{t_1^{(j)}}^{t} v_{\mathrm{down}}^{(\mathrm{jam})}(t)\,\mathrm{d}t \approx L_j - \int_{t_1^{(j)}}^{t} \frac{q_{\mathrm{out}}^{(j)(\mathrm{jam})}(t) - q_{\min}}{\rho_{\max} - \left(q_{\mathrm{out}}^{(j)(\mathrm{jam})}(t)/w_{\max}^{(j)}(t)\right)}\,\mathrm{d}t, \quad t \geqslant t_1^{(j)}, \quad j = 1,2,\ldots \tag{2}$$

with index "$i$" in (1) and "$j$" in (2) for the detectors, whose values at time $t$ have to be used, the indexes "$i$" and "$j$" increase in the direction of the flow, i.e., corresponding the direction of the axis $x$: e.g., $L_m > L_n$ for $m > n$; $L_{i+1}$, $L_j$ are the co-ordinates of the corresponding detectors; $t_0^{(i+1)}$ indicates the time when the upstream jam front has been measured at the detector "$i+1$"; $t_1^{(j)}$ indicates the time when the downstream jam front has been measured at the detector "$j$"; $q_0^{(i)}(t)$ and $w_0^{(i)}(t)$ are the measured flow rate and the averaged vehicle speed at the detectors "$i$" upstream of a wide moving jam; $q_{\text{out}}^{(j)(\text{jam})}$ and $w_{\max}^{(j)}$ are the measured flow rate and the averaged vehicle speed at the detectors "$j$" downstream of the wide moving jam; $q_{\min}$ is the measured flow rate inside the moving jam; $\rho_{\max}$ is the vehicle density inside the moving jam; $v_{\text{down}}^{(\text{jam})}(t)$ and $v_{\text{up}}^{(\text{jam})}(t)$ are the velocities of the downstream and upstream fronts of the moving jam, respectively.

The parameter $\rho_{\max}$ can be calculated directly from the traffic data via the following formula:

$$\rho_{\max} = \frac{1000}{L_{\text{PC}} \cdot A_{\text{PC}} + L_{\text{HGV}} \cdot (1 - A_{\text{PC}})} \left[\frac{\text{vehicles}}{\text{km}}\right] \tag{3}$$

with $L_{\text{PC}}$ being the expected average length of passenger cars (PC) including a (small) average distance between vehicles inside the moving jam (e.g., $L_{\text{PC}} = 7\,\text{m}$) and $L_{\text{HGV}}$ being the average length of heavy goods vehicles (HGV) including a (small) average distance between vehicles inside the moving jam (e.g., $L_{\text{HGV}} = 17\,\text{m}$); $A_{\text{PC}}$ is the fraction of PC and $(1-A_{\text{PC}})$ is the fraction of HGV. These fractions can be determined with the local detector measurements. In formulas (1) and (2), $q_{\min}$ can be set to the mean measured flow rate within the jam. At times when there is no detector within the jam, $q_{\min}$ can be approximated either through the formula (4a) or (4b):

$$q_{\min} = \left(t_1^{(j)} - t_0^{(j)}\right)^{-1} \int_{t_0^{(j)}}^{t_1^{(j)}} q_{\min}^{(j)}(t)\,\mathrm{d}t, \tag{4a}$$

$$q_{\min} = 0. \tag{4b}$$

where "$j$" is the detector used in formula (2).

For the choice of the correct detector "$i$", whose measured data should be used in (1), the following algorithm can be applied. This algorithm will be illustrated for the case shown in Fig. 4(b) where the upstream front of a moving jam has just been registered at the detector "$i+1=k$".

In the beginning, detector $i = k-1$ is used in (1) and the downstream front of the jam is not tracked since it has not reached detector "$k$" yet.

First, we will define the time points when the next detector upstream for the calculation of the velocity of the upstream front of the moving jam has to be used in (1). If the following inequality becomes true:

$$x_{\text{up}}^{(\text{jam})}(t) \leqslant L_{k-1}, \tag{5}$$

the measurements of the detector with index, "$i = k-2$" (Fig. 4(b)) have to be used in formula (1). In the inequality (5) $L_{k-1}$ is the $x$ co-ordinate of the detector with index "$i = k-1$". On the other hand, the upstream front of the jam is registered at detector "$i = k-1$" at the time $t_0^{(k-1)}$ when the upstream front reaches that detector, i.e.,

$$x_{\text{up}}^{(\text{jam})}\left(t_0^{(k-1)}\right) = L_{k-1} \text{ with } x_{\text{up}}^{(\text{jam})}\left(t_0^{(k-1)}\right) = L_k + \int_{t_0^{(k)}}^{t_0^{(k-1)}} v_{\text{up}}^{(\text{jam})}(t)\,\mathrm{d}t. \tag{6}$$

Note that there is always a difference $\Delta$ between the calculated $x_{up}^{(jam)}$ and the real co-ordinate of the upstream front of the moving jam. If, for example, inequality (5) is still false for the calculated upstream front at time $t_0^{(k-1)}$ when that front is already registered at detector $k-1$, the calculated $x_{up}^{(jam)}\left(t_0^{(k-1)}\right)$ is definitely too high. In that case, the algorithm sets $x_{up}^{(jam)}\left(t_0^{(k-1)}\right)$ to $L_{k-1}$. Similarly, the calculated $x_{up}^{(jam)}(t)$ is definitely too low if $x_{up}^{(jam)}(t) \leqslant L_{k-1}$, but the jam's upstream front has not yet been detected by detector "$k-1$" at time $t$. Then, $x_{up}^{(jam)}(t)$ is set to $L_{k-1} + \varepsilon$ where $\varepsilon$ is a small given value (we use $\varepsilon = 1$ m).

Consequently, the choice of the next upstream detector in formula (1) does not depend on the calculated position of the jam's upstream front, but on the registration times of the upstream front at the detectors: Detector "$i = k-m-1$" is used in (1) as soon as the jam's upstream front has been registered by the detector "$k-m$" at time $t_0^{(k-m)}$.

A similar algorithm is applied to choose the detector to be used for the position of the downstream front of the moving jam in formula (2). That formula can first be applied at time $t_1^{(k)}$ when the jam's downstream front is registered at detector "$k$". As soon as that front is registered at the next upstream detector "$k-1$" at time $t_1^{(k-1)}$, the data of detector $j = k-1$ is used in (2).

In a similar manner to the remark of the difference between the real and calculated position of the upstream front of the moving jam described above, the calculated position of the jam's downstream front is corrected according to the registration times of the downstream front at the detectors: If the calculated $x_{down}^{(jam)}(t) > L_{k-p}$, but the downstream front has already been registered at detector "$k-p$", $x_{down}^{(jam)}(t)$ is set to $L_{k-p}-\varepsilon$ ($\varepsilon$ is the above mentioned small value) and if the calculated $x_{down}^{(jam)}(t) < L_{k-p}$, but the jam's downstream front has not yet been registered at detector "$k-p$", $x_{down}^{(jam)}(t)$ is set to $L_{k-p}$.

The case of one wide moving traffic jam detected between the detector "$i = k-1$" and "$i = k$" has been discussed above (Fig. 4(b)). If after the first moving jam—as it happens often in traffic flow—further wide moving jams appear and these wide moving jams are spatially close together with small distances so that there is no detector in between, the model ASDA has to be extended. In this case, the results of empirical investigations of characteristic features of wide moving jams (Kerner and Rehborn, 1996b) can be applied. In particular, the velocity of the downstream front of a wide moving jam is the characteristic parameter. If this velocity was recently measured for a specific wide moving jam, it is applied for the prognosis of the velocity of the downstream front of wide moving jams while this parameter cannot be measured. For the tracking of a wide moving jam which is downstream of the first one, it can also be assumed that the velocity of the upstream front of this jam equals the known characteristic velocity of the downstream front of the first moving jam.

### *3.2. Extensions of ASDA for on-ramps, off-ramps and changing of number of freeway lanes upstream of a moving jam*

In this and the next Section 3.3 all flow rates are related to the flow rate per freeway lane. At an on-ramp the flow rate $q_0^{(i)}(t)$ will be extended by the in-flowing flow rate (distributed on all "$n$" freeway lanes) $q_{on}(t)/n$, if the upstream front of a moving jam has passed the detector "$i + 1$" in the driving direction after the on-ramp (Fig. 5(a)). In other words, the flow rate $q_0^{(i)}(t)$ in (1) should be replaced by

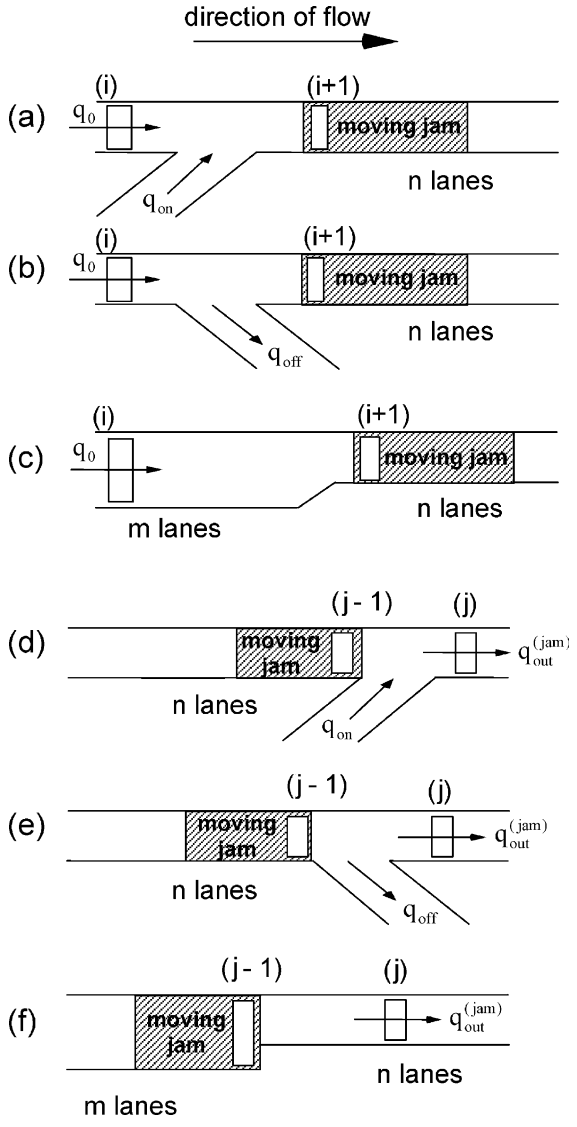


Fig. 5. Extensions of the model ASDA: on- and off-ramps and lane reductions upstream (a)–(c) and downstream (d)–(f) of a moving jam.

$$q_0^{*(i)}(t) = q_0^{(i)}(t) + \frac{q_{\mathrm{on}}(t)}{n}. \tag{7}$$

Correspondingly, when the upstream front of a moving jam passed the detector "$i + 1$" in the driving direction after the off-ramp (Fig. 5(b)), the contribution of the flow rate $q_{\mathrm{off}}(t)/n$ has to be subtracted, i.e., $q_0^{(i)}(t)$ in (1) should be replaced by

$$q_0^{*(i)}(t) = q_0^{(i)}(t) - \frac{q_{\mathrm{off}}(t)}{n}. \tag{8}$$

In the case of a reduction in the number of freeway lanes downstream of the detector "$i$" and upstream of the moving jam the flow rate $q_0^{(i)}(t)$ in (1) has to be applied in relation to the number of lanes (Fig. 5(c)), i.e., $q_0^{(i)}(t)$ in (1) should be replaced by

$$q_0^{*(i)}(t) = \frac{m}{n} q_0^{(i)}(t). \tag{9}$$

In the above cases, instead of the formula (1) for the position of the upstream front of the moving jam the following formula should be used:

$$\begin{aligned} x_{\text{up}}^{(\text{jam})}(t) &= L_{i+1} + \int_{t_0^{(i+1)}}^{t} v_{\text{up}}^{(\text{jam})}(t)\,\mathrm{d}t \\ &\approx L_{i+1} - \int_{t_0^{(i+1)}}^{t} \frac{q_0^{*(i)}(t) - q_{\min}}{\rho_{\max} - \left(q_0^{*(i)}(t)/w_0^{(i)}(t)\right)}\,\mathrm{d}t, \quad t \geqslant t_0^{(i+1)}, \quad i = 1, 2, \ldots \end{aligned} \tag{10}$$

### 3.3. Extensions of ASDA for on-ramps, off-ramps and changing of number of freeway lanes downstream of a moving jam

At an on-ramp the flow rate $q_{\text{out}}^{(j)(\text{jam})}$ in (2) will be reduced by the in-flowing flow rate (distributed on all $n$ lanes) $q_{\text{on}}(t)/n$, if the downstream front of the moving jam has passed the on-ramp (Fig. 5(d)), i.e., the flow rate $q_{\text{out}}^{(j)(\text{jam})}$ in (2) should be replaced by

$$q_{\text{out}}^{*(j)(\text{jam})}(t) = q_{\text{out}}^{(j)(\text{jam})}(t) - \frac{q_{\text{on}}(t)}{n}. \tag{11}$$

Correspondingly, when the downstream front of a moving jam has just passed an off-ramp, the contribution of the flow rate $q_{\text{off}}(t)/n$ (Fig. 5(e)) has to be added, i.e., $q_{\text{out}}^{(j)(\text{jam})}$ in (2) should be replaced by

$$q_{\text{out}}^{*(j)(\text{jam})}(t) = q_{\text{out}}^{(j)(\text{jam})}(t) + \frac{q_{\text{off}}(t)}{n}. \tag{12}$$

In the case of a reduction in the number of freeway lanes downstream of a moving jam and upstream of the detector "$j$" the flow rate $q_{\text{out}}^{(j)(\text{jam})}(t)$ has to be applied in (2) in relation to the number of lanes (Fig. 5(f)), i.e., $q_{\text{out}}^{(j)(\text{jam})}$ in (2) should be replaced by

$$q_{\text{out}}^{*(j)(\text{jam})}(t) = \frac{n}{m} q_{\text{out}}^{(j)(\text{jam})}(t). \tag{13}$$

Thus, formula (2) for the position of the downstream front of the moving jam is replaced by

$$\begin{aligned} x_{\text{down}}^{(\text{jam})}(t) &= L_j + \int_{t_1^{(j)}}^{t} v_{\text{down}}^{(\text{jam})}(t)\,\mathrm{d}t \approx L_j - \int_{t_1^{(j)}}^{t} \frac{q_{\text{out}}^{*(j)(\text{jam})}(t) - q_{\min}}{\rho_{\max} - \left(q_{\text{out}}^{*(j)(\text{jam})}(t)/w_{\max}^{(j)}(t)\right)}\,\mathrm{d}t, \\ & t \geqslant t_1^{(j)}, \quad j = 1, 2, \ldots \end{aligned} \tag{14}$$

## 4. Tracking of synchronized flow with the model FOTO

Similarly to the jam-tracking model ASDA, the positions of the upstream front $x_{\text{up}}^{(\text{syn})}(t)$ and the downstream front $x_{\text{down}}^{(\text{syn})}(t)$ of "synchronized flow" objects are tracked after synchronized flow has first been detected by the model FOTO. It is taken into account that the downstream front $x_{\text{down}}^{(\text{syn})}(t)$ of synchronized flow is usually spatially fixed at the effective location of the bottleneck (e.g., near an on-ramp) on a freeway section while the upstream front is influenced by the upstream supply of vehicles.

The best results of tracking of synchronized flow with FOTO can be achieved, if a detector is close to the effective location of the bottleneck where the downstream front $x_{\text{down}}^{(\text{syn})}(t)$ of the synchronized flow is fixed. In contrast to the downstream front, the upstream front of synchronized flow begins to move upstream after the phase transition from free to synchronized flow has occurred at the bottleneck.

Let us consider a detector "B" where synchronized flow has first been detected at time $t_{\text{syn,B}}$ due to its upstream propagation from the bottleneck. Let us further consider an upstream detector "A" where traffic is still in the phase "free flow" at time $t > t_{\text{syn,B}}$ when traffic at the detector "B" is still in the phase "synchronized flow" (Fig. 6(a)). It is clear that the upstream front of synchronized flow is somewhere between detectors "A" and "B" at time $t$. The flow rate upstream from synchronized flow is computed by taking the incoming flow from the detector "A", $q_{\text{A}}(t)$, and also taking into account the flow rates to the on- and off-ramps.

For the calculation of the upstream front location of synchronized flow at time $t$, $x_{\text{up}}^{(\text{syn})}(t)$, we set the origin $x = 0$ to the location of the detector "B". With the distance $D$ between the detectors "A" and "B", the location of the detector "A" is $x = -D$. Since the upstream front of synchronized flow is somewhere between the detectors "A" and "B", the following inequality holds:

$$-D < x_{\text{up}}^{(\text{syn})}(t) < 0. \tag{15}$$

To estimate the position $x_{\text{up}}^{(\text{syn})}(t)$, two different approaches have been developed and evaluated: (i) the ASDA-like approach (Section 4.1) and (ii) the cumulative flow rate approach (Section 4.2).

### 4.1. The ASDA-like approach for tracking the upstream front of synchronized flow

Let us assume that a synchronized flow at the detector "B" has been registered at $t = t_{\text{syn,B}}$ (Fig. 6(a)). At $t > t_{\text{syn,B}}$ the position $x_{\text{up}}^{(\text{syn})}(t)$ of the front of synchronized flow downstream and free flow upstream between any two neighboring detectors "A" and "B" (the detectors "A" and "B" characterized by the flow rates $q_{\text{A}}(t)$, $q_{\text{B}}(t)$ and the densities $\rho_{\text{A}}(t)$, $\rho_{\text{B}}(t)$, respectively) can be calculated by the ASDA-like formula:

$$x_{\text{up}}^{(\text{syn})}(t) = \int_{t_{\text{syn,B}}}^{t} v_{\text{up}}^{(\text{syn})}(t)\,\mathrm{d}t = \int_{t_{\text{syn,B}}}^{t} \frac{q_{\text{A}}(t) - q_{\text{B}}(t)}{\rho_{\text{A}}(t) - \rho_{\text{B}}(t)}\,\mathrm{d}t, \quad t > t_{\text{syn,B}}. \tag{16}$$

On- and off-ramps are handled in the same way as in the model ASDA. Recall that in the case of the tracking of wide moving jams with the model ASDA it has empirically been shown that the upstream front position of a wide moving jam $x_{\text{up}}^{(\text{jam})}(t)$ (1) is in close agreement with the real jam front position which is found from measurements of the jam propagation through different

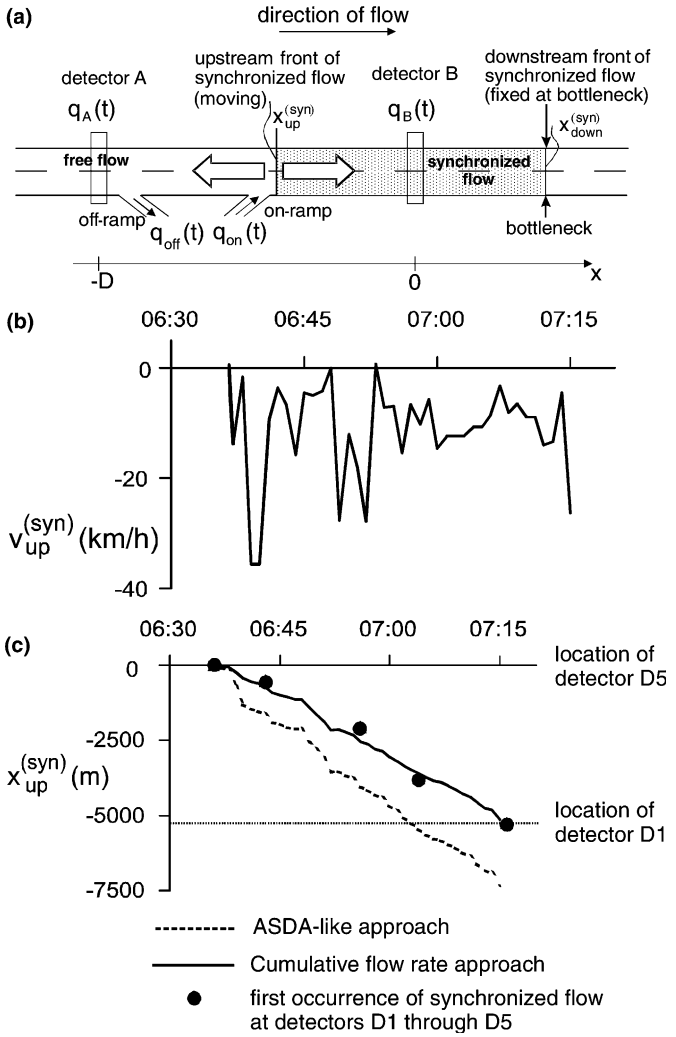


Fig. 6. Tracking of synchronized flow with FOTO: (a) schema of the synchronized flow tracking, (b) the velocity $v_{up}^{(syn)}(t)$ calculated through the formula (16) and (c) the location of the calculated upstream front of synchronized flow $x_{up}^{(syn)}(t)$ for the ASDA-like approach (16) (dashed curve) and for the cumulative flow rate approach (18) and (19) (solid curve). Black points in (c) are related to the measurements of the first occurrence of synchronized flow at the detectors. In (b), (c) data on January 28, 2002, arrangement of detectors in Fig. 3(a).

detectors. However, in the case of the tracking of the front of synchronized flow with the formula (16) we found that the calculated front position $x_{up}^{(syn)}(t)$ sometimes shows a very poor correspondence with measurements of this front at detectors. For example in Figs. 6(b) and (c), the difference in the front positions $x_{up}^{(syn)}(t)$ calculated through the formula (16) (dashed curve in Fig. 6(c)) and found through the measurements (black points in Fig. 6(c)) is sometimes up to 100%. This is because the mean *empirical* velocity of the synchronized flow's upstream front is $\bar{v}_{up}^{(syn)} = -7.9\,\text{km/h}$, however the mean *calculated* velocity through (16) is $\bar{v}_{up}^{(syn)} = -11\,\text{km/h}$.

The reason for this behavior may be the following: The formula (16) assumes that the flow rates and the vehicle densities which are measured at the location "A" are nearly the same as in free flow directly upstream of the location of the front $x_{up}^{(syn)}(t)$. In addition, this formula assumes that measurements of these traffic variables at the detector "B" are nearly the same as these variables directly downstream of the synchronized flow upstream front location, $x_{up}^{(syn)}(t)$. Our empirical investigations show that for free flow upstream of the front location $x_{up}^{(syn)}(t)$ the assumption of (16) is nearly valid. However downstream of the synchronized flow upstream front location $x_{up}^{(syn)}(t)$, i.e., in synchronized flow the formula (16) leads often to an incorrect result. This is linked to a feature of synchronized flow which usually exhibits a very high change in the vehicle density over the road even if the flow rate remains almost a constant value (see Kerner, 2002b).

The error of this ASDA-like approach decreases with smaller distances between the detectors and shorter measurement intervals. An important advantage of this approach is that it works without any parameter validation through the use of the measured traffic data only.

### 4.2. Cumulative flow rates approach for tracking the upstream front of synchronized flow

Empirical observations have shown that there is a nearly linear correspondence between the upstream front position $x_{up}^{(syn)}(t)$ of synchronized flow (Fig. 6(c), black points) and the change of the cumulated number of vehicles between the detectors "A" and "B" that occurred after the time $t_{syn,B}$. This change is the difference $\Delta M_{total}$ of the cumulative flow rate passing the detector "B" and the cumulative flow rate into the region of synchronized flow which is influenced by the flow on the main road measured at the detector "A" and the on- and off-ramps between the detectors "A" and "B":

$$\Delta M_{total}(t) = \int_{t_{syn,B}}^{t} q_B(t)\,dt - \int_{t_{syn,B}}^{t} (q_A(t) + q_{on}(t) - q_{off}(t))\,dt, \quad t > t_{syn,B}. \tag{17}$$

The flow rates in (17) are the total flow rates across the whole cross sections. $\Delta M_{total}(t)$ is the net number of vehicles leaving the road section between the detectors "A" and "B". When the number of vehicles between the detectors increases, $\Delta M_{total}(t)$ is negative. To make the FOTO formulas for the determination of $x_{up}^{(syn)}(t)$ independent of the number of lanes $n$, $\Delta M_{total}(t)$ is "normalized" to the traffic volume per lane, $\Delta M_{lane}(t)$, which will further be used as $\Delta M(t)$:

$$\Delta M(t) = \Delta M_{lane}(t) = \frac{\Delta M_{total}(t)}{n}. \tag{18}$$

The correspondence between $x_{up}^{(syn)}(t)$ and $\Delta M(t)$ has been found empirically to be approximately a linear function:

$$x_{up}^{(syn)}(t) = \mu \Delta M(t), \tag{19}$$

$\mu$ is a constant, $x_{up}^{(syn)}(t)$ is the front position relative to the detector "B" (in meters), the unit of $\Delta M(t)$ is (veh./lane). However, this is an average behavior of the upstream front. When measurements of $\Delta M(t)$ are inserted into (19), the calculated front position $x_{up}^{(syn)}(t)$ (19) can sometimes contradict condition (15). In this case, the calculated value $x_{up}^{(syn)}(t)$ (19) is adjusted according to (15), i.e., if the calculated value $x_{up}^{(syn)}(t) > 0$, it is set to zero, and if the calculated value $x_{up}^{(syn)}(t) \leqslant -D$, it is set to $-D + \varepsilon$, where $\varepsilon$ is the above mentioned small value, $\varepsilon \ll D$.

For the bottleneck near the detector D6 (Fig. 3(a)) it has empirically been found that the mean value $\mu = 33$ (m/veh.) can be used in (19). For different empirical examples at different bottlenecks of the sections of the freeway A5 under consideration a variation of $28 < \mu < 40$ has been found. Nevertheless we have used the constant value of $\mu = 33$ (m/veh.) in the FOTO application. This shows good results for the tracking of the synchronized flow because a possible mistake in this constant is about 15%. However, the constant $\mu$ in (19) might be different for bottlenecks at other freeway sections. Thus, in these cases the constant $\mu$ in (19) should be validated based on historical empirical data.

An example of the application of the formula (19) for the tracking of the synchronized flow is shown in Fig. 6(c) (solid curve). The example was done with a reduced infrastructure where only data from D1, D5 and D5-off are used. The times of the phase transitions measured directly at the detectors D1, D2, D3, D4 and D5 are shown as a reference with black circles. In comparison to the positions calculated by the ASDA-like formula (dashed curve in Fig. 6(c), error 100% at 6:56: the upstream front of synchronized flow supposed to be at −4.0 km, is in reality at −2.0 km), the positions from the cumulative flow rate formula (19) match the actually measured phase transitions at the detectors (black points in Fig. 6(c)) much better.

This approach of the cumulative flow rates allows the determination of the upstream front of the synchronized flow in good accordance to the real propagation. An additional parameter $\mu$ (19) is needed which is valid for a specific bottleneck. Recall that an empirical determination of the parameter $\mu$ is only possible in good measurement infrastructures with many detectors. Therefore the approach based on cumulative flow rates is less optimal in network installations with larger detector distances and measurement intervals.

### 4.3. FOTO in the case of several detectors and dissolving synchronized flow

So far we have discussed the tracking of the upstream front of synchronized flow between a detector "A" where traffic is still in the state "free flow" and a detector "B" where synchronized flow has initially been detected. Once the upstream front of the synchronized flow has reached the detector "A" at a time $t_{\mathrm{syn,A}}$, the further propagation of synchronized flow can be tracked by monitoring the traffic volume since $t_{\mathrm{syn,A}}$ between a next upstream detector "C" and the detector "A". With the new detector distance $D^*$ between the detectors "C" and "A", the same method as for the tracking of the upstream front between the detectors "A" and "B" is used. However, this method can only be used as long as traffic at the detector "A" is in the state "synchronized flow", i.e., no wide moving jam occurred at the detector "A".

When the upstream supply of vehicles flowing into the area of synchronized flow from the main road decreases, the upstream front of synchronized flow can begin to move downstream until it reaches the bottleneck and the synchronized flow is dissolved. In the course of this process, the situation can occur that the upstream front of synchronized flow moves downstream across the detector "A" at time $t_{\mathrm{free,A}}$ but traffic is still in the synchronized flow state at the next downstream detector "B". In this case, the same methods as for the tracking of the upstream front of the expanding synchronized flow between the detectors "A" and "B" is used. The difference is that in (17) the time $t_{\mathrm{free,B}}$ should be replaced by the time $t_{\mathrm{free,A}}$ and the resulting coordinate of the upstream front of synchronized flow $x_{\mathrm{up}}^{(\mathrm{syn})}(t)$ (19) should be replaced by $x_{\mathrm{up}}^{(\mathrm{syn})}(t) = -D + \mu\Delta M(t)$.

## 5. Online application and evaluation of the models FOTO and ASDA

### 5.1. Results of the online application of FOTO and ASDA

In the application FOTOwin both the models FOTO and ASDA are integrated. For operation at the TCC in the federal state Hessen near Frankfurt the data exchange is performed with a central information distributor, which manages the data of the detectors. The models have been installed first on the freeway A5 near the variable message signs equipment between intersection "Westkreuz Frankfurt" and the intersection "Anschlussstelle Friedberg" in both directions. A more detailed consideration of the implementation of the FOTOwin software has been considered in (Kerner et al., 2001b).

FOTOwin has the possibility to show the traffic objects over a longer time interval to investigate the spatial–temporal movement of the objects: A space-time diagram gives a history of the traffic objects (Fig. 7). The $x$-axis is the time and the $y$-axis the position on the road. In the representation, moving jam objects are shown in black and synchronized flow objects are shown in gray. The infrastructure is shown with horizontal lines for the detectors' positions. Using this space-time diagram, the movement of the different traffic objects in time and space can directly be seen.

It should be noted that in each case *the reference* for a correct or false classification of the traffic phases "synchronized flow" and "wide moving jam" with the model FOTO is made based on the following approach: A comparison of the traffic phases which follow from the objective criteria for the traffic phases (see Section 1) based on the local measurements only (i.e., without the application of the model FOTO) with the results of the traffic phase reconstruction with the model FOTO is made. Naturally the latter is only possible with high quality results if the detector distances are small (about or less than 1000 m). In this case an interpolation of the minute speed values of the detectors give a spatial–temporal structure of congested patterns where the traffic phase through the objective criteria can be distinguished. Most results of the application FOTO and ASDA below will be presented for the sections of freeway A5 where at about 30 km length about 30 detectors exist, i.e., the mean detector distance is 1 km.

For the example shown in Fig. 7 time–space plots of the detector data with interpolation between detectors look very similar to the results of the models FOTO and ASDA shown here. On the one hand, it shows a high quality of the approach. On the other hand, if the distance between detectors is not small then the mentioned data interpolation makes a considerable mistake in comparison with the real spatial–temporal pattern. We will see below that in contrast to this data interpolation, the models FOTO and ASDA allow us to make a high quality tracking of spatial–temporal congested patterns even at relatively high distances between detectors. Thus, an advantage of the models FOTO and ASDA becomes more visible at less ideal detector infrastructures.

For the evaluation of the models FOTO and ASDA the application is tested in strongly reduced configurations: traffic data of several detectors have been omitted. In the reduced configuration the models FOTO and ASDA (Fig. 7(c) and (d)) reproduce the wide moving jams and the synchronized flow with good accordance in comparison to Fig. 7(a) and (b) where all detectors have been used. In particular, a possible dissolving of the objects "wide moving jam" and "synchronized flow" which occurs between detectors can be predicted, i.e., even when the objects cannot

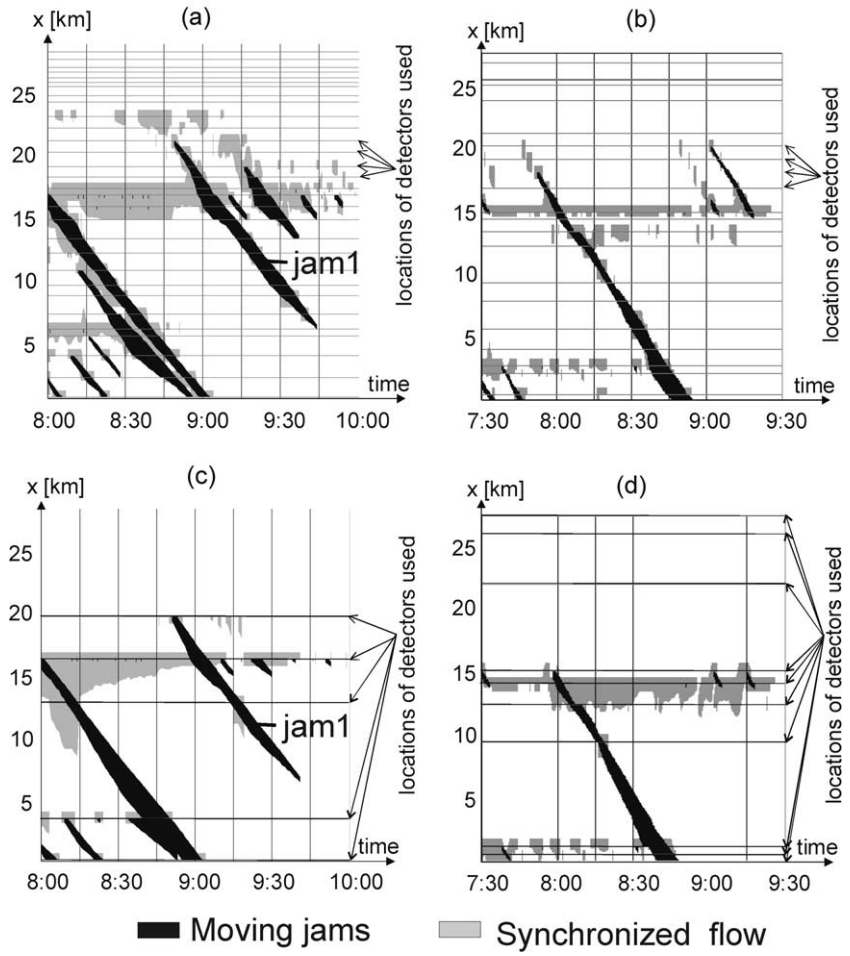


Fig. 7. Results and evaluation of FOTO and ASDA application: space-time diagrams of spatial–temporal congested patterns. (a) A5-South on 17th March, 1997 where all available 31 detectors are used. (b) A5-North on 11th August, 2000 where all available 30 detectors are used. (c) Related to (a) where 5 instead of 31 detectors are used. (d) Related to (b) where 10 instead of 30 detectors are used.

be measured. An example is shown in Fig. 7(a) where a wide moving jam "jam1" dissolves at $t = 9{:}44$. This moving jam dissolving is predicted through the jam tracking in the model ASDA in the reduced detector configuration at $t = 9{:}41$ (Fig. 7(c)), i.e., when the moving jam cannot be measured by the detectors.

Another example where the limitation of the spatial propagation of the object "synchronized flow" is predicted through the synchronized flow tracking in the model FOTO when the position of the upstream front of synchronized flow cannot be measured is shown in Fig. 7(d). In this case, a location of the upstream front of synchronized flow is predicted to be located between 10 and 15 km (in the agreement with the result in Fig. 7(b) where the full detector configuration is used) whereas the measurements between these freeway locations are not used in the model FOTO in

Fig. 7(d). A statistical evaluation of different reduced detector configurations is described in Section 5.3.

### 5.2. Online application of FOTO and ASDA in other freeways

FOTOwin has been installed for the whole freeway network in Hessen with estimated 800 detectors and 850 km of freeway network. The models have therefore to cope with different detector infrastructures (distances between detectors up to 10 km), different measurement intervals

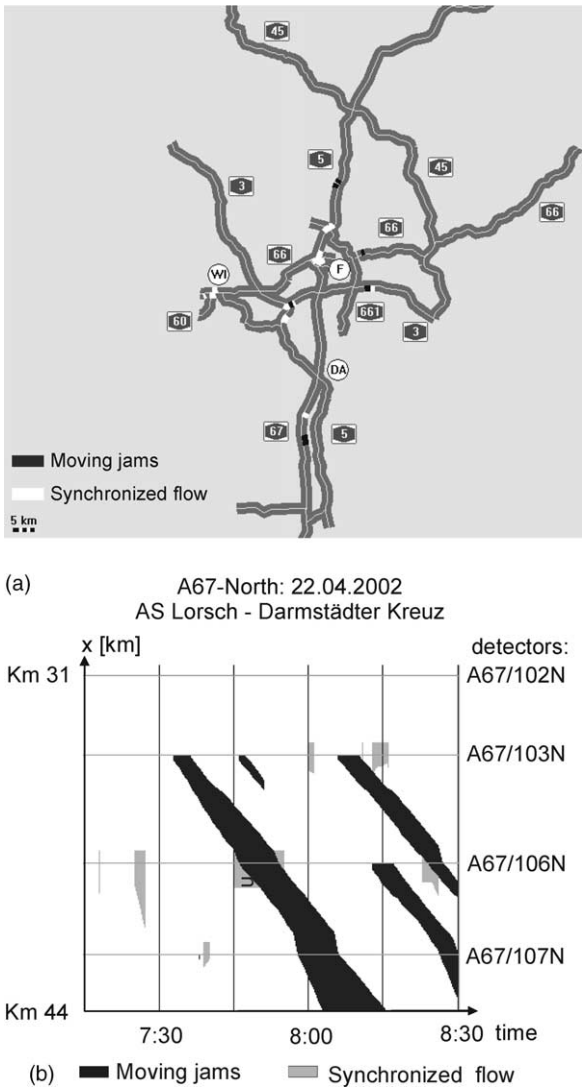


Fig. 8. Results of FOTO and ASDA application in the Rhein/Main area on several freeways: (a) schema of the area with results of data from 22nd April, 2002 at 8:00, (b) space-time diagram for the freeway A67-North (data from 22nd April, 2002).

(1 and 5 min) and with different kinds and mixtures of local, regional, long distance and leisure traffic. Fig. 8 (a) illustrates FOTO and ASDA results in the Rhein/Main-area: positions of wide moving jams (in black color) and regions of synchronized flow (in white color) are marked on the different freeway sections.

Fig. 8(b) shows a space-time diagram (22nd April, 2002: 07:15–08:30) for the freeway A67-North between intersection "AS Lorsch" (km 44) and intersection "Darmstädter Kreuz" (km 31) within the net in Fig. 8(a) which has a larger percentage of long distance traffic than the freeway A5 located near the city of Frankfurt. In an example of the FOTO and ASDA-application (Fig. 8(b)) three wide moving jams propagating upstream can be seen on the 13 km stretch with four detectors at 3–5 km distance. Note, that because the detectors are in this case far away from the bottlenecks (only a detector A67/106 N is close to on- and off-ramps) on the two-lane (in one-way) freeway the regions of synchronized flow emerging at those bottlenecks cannot be detected and tracked. On the other hand, the wide moving jams are tracked with ASDA at relatively large detector distances of 3–5 km. The characteristic value of the velocity of the downstream front propagation is here −16 km/h at a maximum observation distance of 8,1 km between the detectors A67/103 N and A67/107 N. This is in good accordance to the results on the freeway sections of A5 near Frankfurt.

Additional examples of the ASDA and FOTO application in freeways near Magdeburg and near Munich (both Germany) are shown in Figs. 9 and 10, respectively. The results of the ASDA and FOTO application in these examples are qualitatively the same as the results of the on-line application for freeways in Hessen (Figs. 7 and 8).

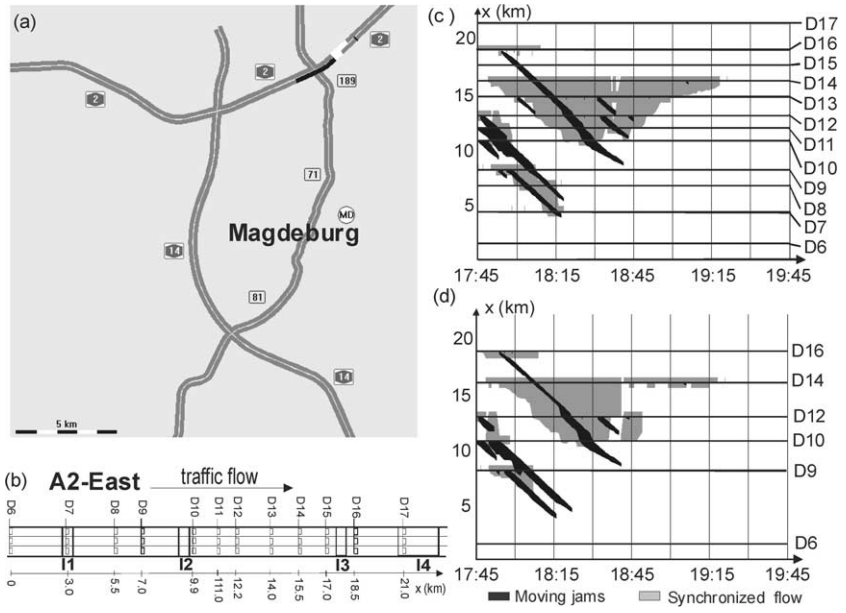


Fig. 9. Results and evaluation of FOTO and ASDA application in freeways near Magdeburg: (a), (b) freeways schemas, (c) all available detectors are used and (d) reduced detector infrastructure. In (c), (d) A2-East, data on 13th September, 2002.

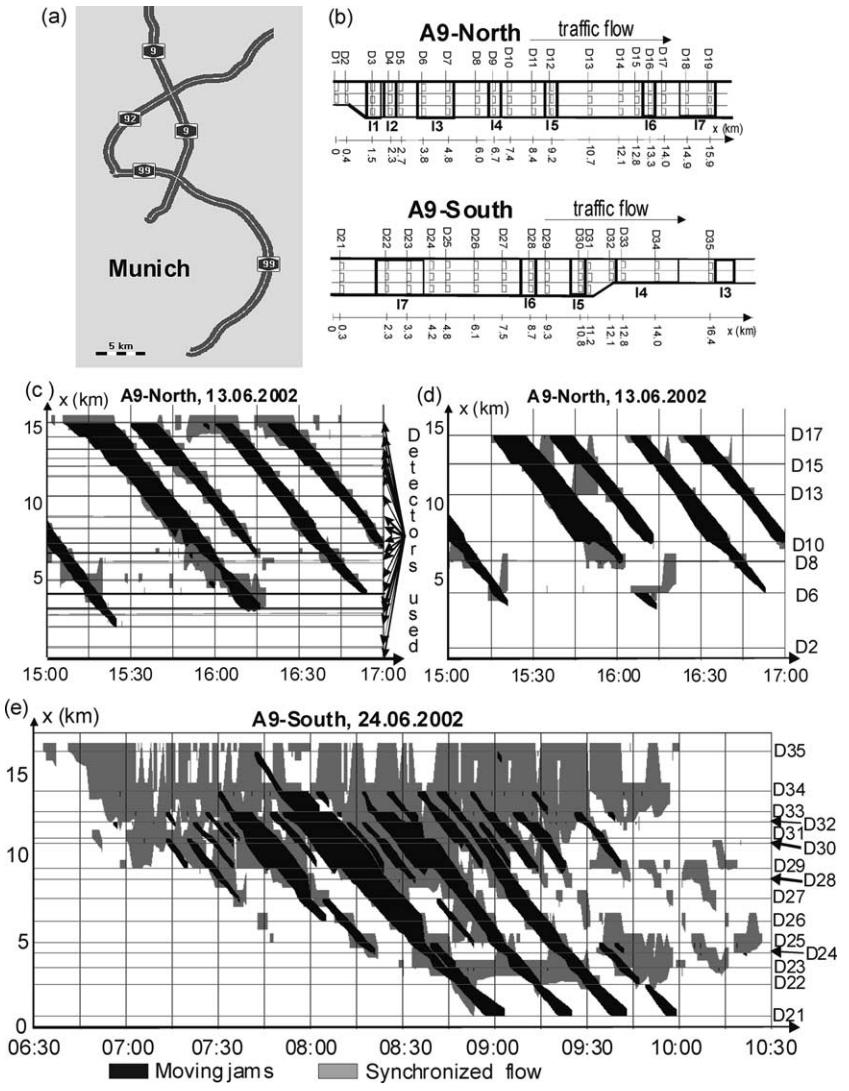


Fig. 10. Results and evaluation of FOTO and ASDA application in freeways near Munich: (a), (b) freeways schemas, (c) all available detectors are used, (d) reduced detector infrastructure. In (c), (d) A9-North, data on 13th June, 2002. (e) Complex spatial–temporal traffic pattern on A9-South, data on 24th June, 2002.

### 5.3. Statistical evaluation of results for different reduced detector configurations

For the online field trial made from 13th June, 2000 until 22nd October, 2000 results of the statistical evaluation of the models FOTO and ASDA under different reduced detector configurations have been performed in (Kniss, 2000). This evaluation has shown a very high practical relevance of the approach FOTO and ASDA for the recognition and tracking of spatial–temporal congested patterns on freeways.

Here we will make a more extended evaluation of FOTO and ASDA. The main question which we would like to answer is the following: Which reduced detector configuration allows us to make the best possible quality recognition and tracking of spatial–temporal congested patterns?

To find out about cost-efficient measurement infrastructures that still lead to good results with FOTO and ASDA, the following approach has been chosen: The full detector configuration at the A5-North (Fig. 11, A5-North: Full) is reduced to only 23% of the detectors (77% of the measurements have been omitted for the models FOTO and ASDA). These omitted detectors have been used for the evaluation of the results performed with reduced detector configurations.

The remaining 23% detectors are chosen differently, i.e., two different reduced detector infrastructures have been studied: (1) Firstly, the detectors between freeway intersections (between potential bottlenecks) plus the detectors at on- and off-ramps have been used (the reduced detector infrastructure "Min1" in Fig. 11 and Table 2). (2) Secondly, only main road detectors which are located close to the intersections without detectors at ramps have been chosen (the reduced detector infrastructure "Min2" in Fig. 11 and Table 2). Both configurations "Min1" and "Min2" are oriented at complete balancing of vehicle numbers, i.e., there are no large detector distances with undetected on- and/or off-ramps in between.

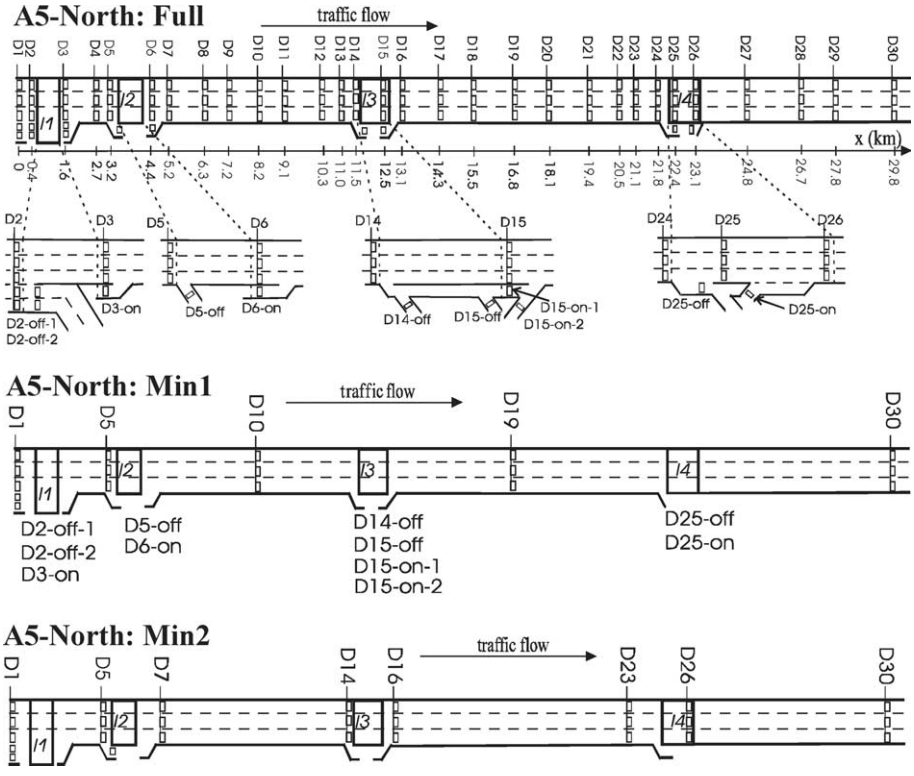


Fig. 11. Three different detector configurations: the configuration "Full" with all available 30 detectors on the main road, the configuration "Min1" with 5 main road detectors and detectors at on- and off-ramps and the configuration "Min2" with 8 main road detectors.

Table 2
Detector infrastructure configurations on A5-North: "Full", "Min1", "Min2" (Fig. 11)

| Detector configuration | A5-North |
|---|---|
| "Full" | 30 main road detectors and detectors at on- and off-ramps in the following intersections "Anschlussstelle Friedberg" (2 detectors), "Bad Homburger Kreuz" (4 detectors), "Nordwestkreuz" (2 detectors), "Westkreuz" (3 detectors) |
| "Min1" | 5 main road detectors and detectors at on- and off-ramps in the following intersections "Anschlussstelle Friedberg" (2 detectors), "Bad Homburger Kreuz" (4 detectors), "Nordwestkreuz" (2 detectors), "Westkreuz" (3 detectors) |
| "Min2" | 8 main road detectors |

Table 3
Objects and detection rates in each the two configuration for objects depending on their lifetime

| Type of object | Objects full configuration | Min1 | Min1 in % of full configuration | Min2 | Min2 in % of full configuration |
|---|---|---|---|---|---|
| Wide moving jam | 4826 | 2029 | 42 | 2504 | 51.9 |
| Wide moving jam > 5 min | 1632 | 859 | 52.6 | 996 | 61 |
| Synchronized traffic flow | 10482 | 2755 | 26.3 | 4318 | 41.2 |
| Synchronized traffic flow > 5 min | 2933 | 977 | 33.3 | 1870 | 63.8 |

Table 3 shows the number of detected objects "synchronized flow" and "wide moving jam" in these three configurations during the field trial. All following analyses use 15.300 empirical objects (≈4.800 "wide moving jam" objects and ≈10.500 "synchronized flow" objects) which have occurred on the section of the freeway A5-North from 13th June, 2000 until 22nd October, 2000. The mean life duration the object "wide moving jam" is ≈9 min whereas the mean life duration of the object "synchronized flow" is ≈6 min.

It is important to note that for both configurations "Min1" and "Min2" the detection rate for wide moving jams is close to 50% of the case of the "Full" detector configuration, while for the synchronized flow the detector configuration "Min2" detects almost 42% of the "Full" detector configuration and the detector configuration "Min1" only 26%. In other words, choosing the detector configuration in a more optimal way ("Min2") in the shown example only 23% of all detectors are sufficient to detect and track ≈50% of both kinds of traffic objects.

The detection rate for wide moving jams increases slightly from 51.9% to 61% in the detector configuration "Min2" if only longer living objects (lifetime longer than 5 min) are considered (Table 3). The detector configuration "Min1" shows a similar increase. This effect is more significant for synchronized flow objects: the detector configuration "Min2" shows 50% higher detection rates for lifetimes above 5 min. In the detector configuration "Min1", however, this detection rate only increases from 26.3% to 33.3%. The detector configuration"Min2" detects twice as many (about 2/3 of the objects detected and tracked by the "Full" detector configuration) longer living synchronized flow objects than "Min1" (about 1/3 of the objects detected and tracked by the "Full" detector configuration).

Table 4
Delay time of all detected objects for A5-North

| Type of object | Min1 in % of full configuration | Min2 in % of full configuration |
|---|---|---|
| Wide moving jam: delay time | 56.97 | 60.84 |
| Synchronized flow: delay time | 27.2 | 63.7 |

In the above analysis, each detection of a "wide moving jam" or "synchronized flow" object is weighted in the same way. For example whether a 10-min-living wide moving jam is detected already after the second minute or only after the ninth minute makes no difference in the detection rate. Moreover, no distinction is made between differently sized objects: The detection of a 2 km-wide moving jam counts as much as the detection of a 500 m-wide moving jam. To account for these differences, Table 4 gives a comparison of the two configurations in terms of delay time for motorists caused by the traffic objects detected over time by the two configurations.

The delay time is calculated by the contributions of each single object with its separate width and average speed for the whole A5 stretch at each single minute cycle. For the 4-month field trial the detector configurations "Min1" and "Min2" detect almost two thirds of the delay time values due to an occurrence of a wide moving jam. For synchronized flow objects the detector configuration "Min1" shows only one third of the total (for the "Full" configuration) delay time values due to an occurrence of the synchronized flow whereas the detector configuration "Min2" is still at two third of the total delay time values for synchronized flow objects. Thus, only 23% of the detectors estimate up to two third of the full measurement infrastructure, but the advantage of the detector configuration "Min2" over "Min1" is smaller for "wide moving jams" and bigger for "synchronized flow".

An illustration of these conclusions for data on 19th October, 2000 at the A5-North is shown in Fig. 12. The configuration "Min2" indeed allows to detect synchronized flow objects with higher accuracy than "Min1" (Fig. 12(a)–(c)). For this reason, the "Min2" travel time comes closer to the "Full" travel time (Fig. 12(d)). After 17:00 both reduced configurations "Min1" and "Min2" are less accurate in comparison with the "Full" configuration because at km 12–15 new wide moving jams occur which are not detected. In a free flow condition a travel time would be about 15 min (at 120 km/h), i.e., in the congested condition in Fig. 12 it is nearly twice as much as in free flow.

### 5.4. Evaluation of FOTO and ASDA with respect to the suitability of the infrastructure

A performance analysis during the field trial of the FOTOwin application under different infrastructures and weather conditions has shown that the models perform without any validation of model parameters in different environmental and traffic conditions. It has been found that both wide moving jams and regions of synchronized flow can best be tracked by the models FOTO and ASDA when there are no effective locations of bottlenecks between two consecutive detectors (Table 5, (i)). In this case, the distance between two detectors can be up to 10 km without a big loss in quality. Even if the distance is 10–20 km, moving jams can still be tracked well while the suitability for synchronized flow is medium (Kerner et al., 2001c).

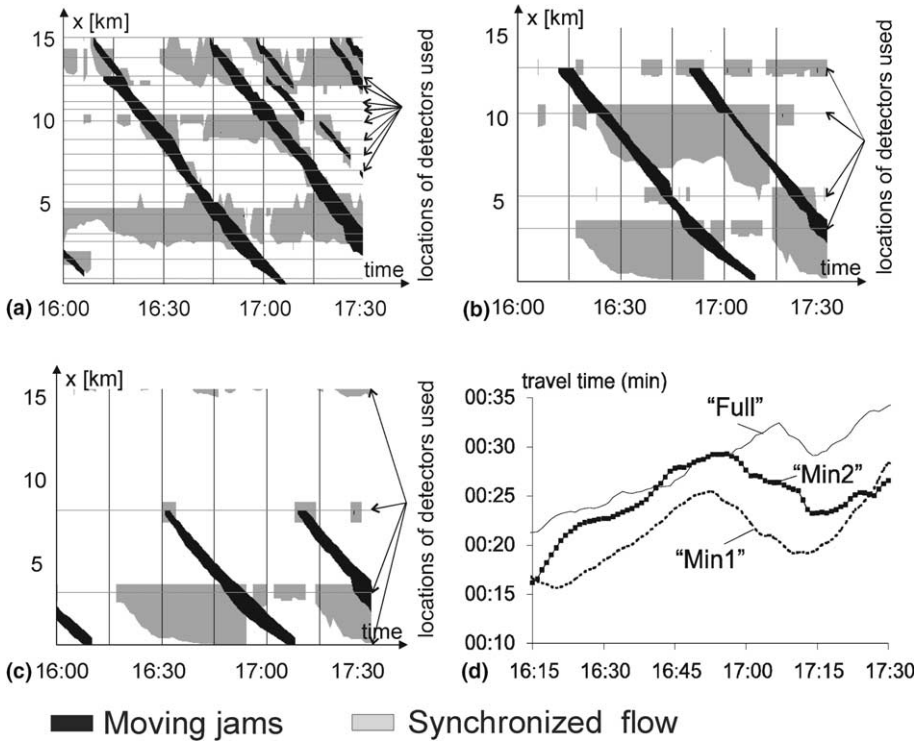


Fig. 12. Evaluation of FOTO and ASDA for different detector configurations in Fig. 11: (a)–(c) space-time diagrams for the "Full" (a), "Min2" (b) and "Min1" (c) detector configurations. (d) Travel time at the whole 30 km stretch of the A5-North for "Full" (black line), "Min1" (thin dotted line) and "Min2" (thick dotted line) detector configurations.

Table 5
Suitability of the infrastructure for the models FOTO and ASDA

| Case | Distance between detectors (km) | Suitability for moving jams | Suitability for synchronized flow |
|---|---|---|---|
| (i) No bottlenecks between detectors | <10 | Very good | Very good |
| | 10–20 | Very good | Medium |
| (ii) Bottlenecks between detectors | <3 | Very good | Medium |
| | 3–10 | Medium | Bad |
| | 10–20 | Bad | Bad |
| (iii) Detectors both away from bottlenecks and directly upstream of the bottlenecks | <3 | Very good | Very good |
| | 3–10 | Good | Good |
| | 10–20 | Medium | Medium |

When there is a bottleneck between two consecutive detectors, the results highly depend on whether or not traffic is detected in the vicinity of the bottleneck (Table 5, (ii) and (iii)). This is linked to the empirical fact that as opposed to wide moving jams, synchronized flow mostly remains near a bottleneck. Synchronized flow can only be detected if there is at least one detector in the area close to the bottleneck where the phase transition from free to synchronized flow

occurs (for example detectors D5, D14, D23 in the detector configuration "Min2", Fig. 11). When the detector is further upstream from the bottleneck, the synchronized flow is only detected after its upstream front has reached that detector. Since upstream fronts of synchronized flow often move slowly, even a distance of 3–5 km between the detector and the effective location of the bottleneck can result in a delay of half an hour or more until the synchronized flow is detected—if the upstream front of the synchronized flow reaches the detector at all (see especially the detector configuration "Min1" with detectors D10 and D19, Fig. 11).

## 6. Conclusions

The models FOTO and ASDA allow to reconstruct and to track the main spatial–temporal features of congested patterns in freeway traffic, in particular at freeway bottlenecks. These models perform without any validation of model parameters in different environmental and infrastructure situations.

The discussion of results show the features of FOTO and ASDA with examples which are based on a stationary infrastructure and their cyclic aggregated measurements. The models FOTO and ASDA have been installed at the TCC Hessen (traffic control center near Frankfurt, Germany). It has been shown that the models are very reliable without any validation of model parameters in all different situations: most traffic objects in congested regime ("wide moving jam" and "synchronized flow") can be reconstructed and tracked even at infrastructures with less detection. The dissolution of the objects "wide moving jam" and "synchronized flow" which occurs between detectors can be predicted, i.e., even when the objects cannot be measured. Choosing optimal detector positions with regard to the effective locations of bottlenecks gives a large potential for saving roadside infrastructure investments: It has been shown in a four month field trial that with only 23% of all given measurements at the A5 nearly 60% of the relevant information can be reconstructed (Table 4).

The online description of the current traffic state and the tracking of traffic objects "wide moving jam" and "synchronized flow" based on stationary measurements performed by the models FOTO and ASDA gives successful opportunities to reconstruct and to track realistic traffic patterns for traffic control centers as basic information for all kinds of traffic management.

## Acknowledgments

We would like to thank the HLSV (Hessisches Landesamt für Strassen- und Verkehrswesen: Hessen ministry for road and traffic) for the possibility of a field trial and the help in the preparation of the data.

## Appendix A. Extended set of fuzzy rules

The basic set of fuzzy rules discussed above allows us to perform an accurate classification of the traffic phase in almost all cases. For the recognition of wide moving jams, those rules use the

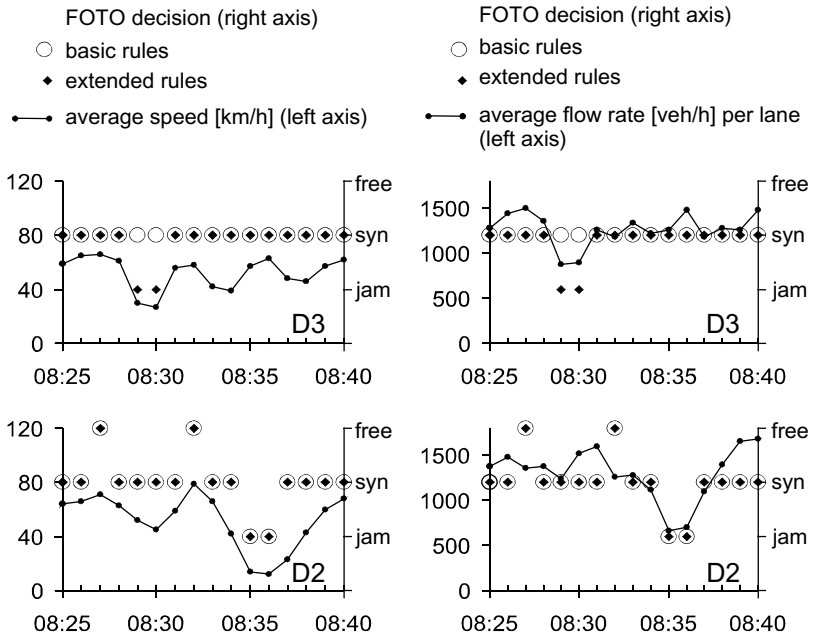


Fig. 13. Comparison of the FOTO decision with basic (circles) and extended fuzzy logic (squares). Data for the A5-South, January 28, 2002. The detector arrangement is in Fig. 3(a).

fact that both the flow rate and the average vehicle speed are at a low level inside a wide moving jam. However, there are cases when the flow rate drops sharply inside a moving jam, but remains at a relatively high value. If this flow rate remains above 800 veh./h, it has a higher degree of membership in the fuzzy set "high" than in the fuzzy set "low" with the basic fuzzy rules (Fig. 2). Fig. 13 shows such an example: The drop in the average vehicle speed and flow rate at detector D3 at 8:29 is classified as "synchronized flow" by the basic rules because the flow rate does not get lower than 880 veh./h at 8:29. The correct classification would be "wide moving jam": This wide moving jam propagates upstream and reaches D2 at 8:35 where it is correctly classified even with the basic fuzzy rules.

This problem cannot be solved by simply using different membership functions for the flow rate because flow rates of 880 veh./h can also occur in synchronized flow. Analyses suggest that there is a certain range of vehicle speeds and flow rates where a distinction between "synchronized flow" and "wide moving jam" can be made by considering recent changes in time of the flow rate and the average vehicle speed in addition to the current values of the flow rate and the speed. This was realized with an extended set of 13 fuzzy rules that classifies the moving jam in Fig. 13 correctly.

The range of vehicle speeds where the value change of the speed has to be considered is between the fuzzy sets "low" and "medium" in the basic fuzzy rules. Therefore, these fuzzy sets have been split into the three new sets "very low", "low" and "medium" in the extended fuzzy logic (Fig. 14(a)). The fuzzy set "high" remains the same as in the basic fuzzy logic (Figs. 2(a) and 14(a)). The set "low" in the new fuzzy logic is the range of vehicle speeds where the value change of

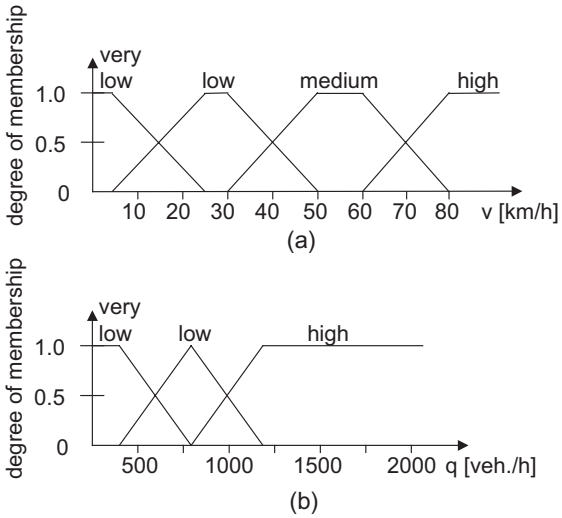


Fig. 14. Fuzzification of the input variables in FOTO with the extended fuzzy logic: (a) "vehicle speed" and (b) "flow rate".

the speed is considered. Similarly, the flow rate is classified in the new sets "very low", "low" and "high" in the extended fuzzy logic, where "low" is the range where the value change of the flow rate is considered (Fig. 14(b)).

In the case when the vehicle speed is "low" and the flow rate is "low", it is taken into account that the upstream front of a wide moving jam is accompanied by a sharp drop in both the vehicle speed and the flow rate whereas the downstream front of the moving jam is accompanied by a sharp rise in the vehicle speed and the flow rate at a detector. The relative changes in the flow rate and the vehicle speed are used as additional input to the fuzzy logic circuit. To account for fluctuations in the measured vehicle speed and the flow rate, the maximum differences in the flow rate and in the speed within a higher time interval $\Delta t$ before the last measurement is considered rather than taking just these differences between the last two measurements.

Usually a discrete sequence of measurements is available for FOTO. Let us further consider two such consecutive moments of time $t_0$ and $t^*$ ($t_0 > t^*$) within the interval $\Delta t$. If the flow rate has dropped between the time $t^*$ and the time $t_0$, i.e., $q(t_0) < q(t^*)$, the difference between the measurement, $q(t_0)$ at the time $t_0$, and the maximum value measured during the whole time $\Delta t$, $\max_t(q(t))$, is considered as a value "diff" in Fig. 15(a). If the flow rate has risen between $t^*$ and $t_0$, the difference between the measurement $q(t_0)$ and the minimum flow rate measured during the whole time $\Delta t$, $\min_t(q(t))$, is considered as a value "diff" in Fig. 15(b).

The input variable $d_q(t_0)$ to the fuzzy-logic circuit is the change of the flow rate (diff) relative to $\max_t(q(t))$ if the flow rate has dropped and relative to $q(t_0)$ if the flow rate has risen, i.e.,

$$d_q(t_0) = \frac{q(t_0) - \max\limits_t(q(t))}{\max\limits_t(q(t))}, \quad \text{if } q(t_0) \leqslant q(t^*) \quad \text{and} \quad d_q(t_0) = \frac{q(t_0) - \min\limits_t(q(t))}{q(t_0)},$$

$$\text{if } q(t_0) > q(t^*).$$

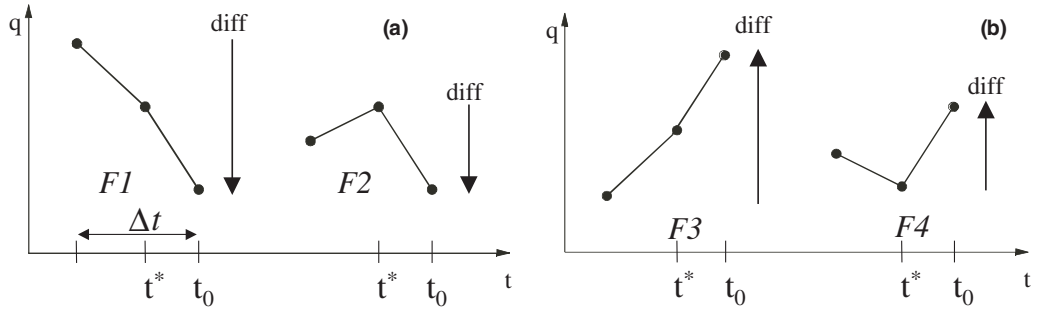


Fig. 15. The difference in the flow rate "diff" (down-arrows for "diff" < 0 and up-arrows for "diff" > 0) when within $\Delta t$ there are three measurements: (a) the flow rate has dropped in the last interval (situations F1 and F2), (b) the flow rate has risen in the last interval (F3 and F4).

The same method is used to calculate the relative change of the vehicle speed, $d_v(t_0)$:

$$d_v(t_0) = \frac{v(t_0) - \max_t(v(t))}{\max_t(v(t))}, \quad \text{if } v(t_0) \leqslant v(t^*) \quad \text{and} \quad d_v(t_0) = \frac{v(t_0) - \min_t(v(t))}{v(t_0)},$$

$$\text{if } v(t_0) > v(t^*).$$

Another input variable to the extended fuzzy-logic circuit is the ratio $c(t_0) = \frac{d_v(t_0)}{d_q(t_0)}$ of the relative change of the vehicle speed to the relative change of the flow rate. In the case of negative $d_v(t_0)$ and negative $d_q(t_0)$ (a potential phase transition either from free flow or from synchronized flow to a wide moving jam), a low value of $c(t_0)$ indicates that the drop in the flow rate was relatively stronger than the drop in the vehicle speed. Analyses have shown that this is a sign that the phase transition to a wide moving jam did indeed occur whereas a high value of $c(t_0)$ indicates that it is less likely that the transition has occurred. The membership functions of the additional variables $d_v(t_0)$, $d_q(t_0)$ and $c(t_0)$ (Fig. 16) have been chosen empirically by comparing the quality of the results achieved with different functions.

In the case of a possible transition from a wide moving jam to another traffic phase (free flow or synchronized flow), i.e., when both $d_v(t_0)$ and $d_q(t_0)$ are positive, a similar analysis concerning $c(t_0)$ has been made. If the rise in the vehicle speed is relatively sharper than the rise in the flow rate, i.e., if $c(t_0)$ is high, traffic is likely to have remained in the "wide moving jam" phase while a transition to another traffic phase is likely to have occurred if $c(t_0)$ is low.

As a result, the whole set of fuzzy rules for the online determination of traffic phases based on local detector measurements consists of 13 rules:

(1) If the vehicle speed is "high", the traffic phase is "free flow".
(2) If the vehicle speed is "medium", the traffic phase is "synchronized flow".
(3) If the vehicle speed is not "high" and the flow rate is "high", the traffic phase is "synchronized flow".
(4) If the vehicle speed is "very low", the traffic phase is "wide moving jam".
(5) If the vehicle speed is "low" and the flow rate is "very low", the traffic phase is "wide moving jam".

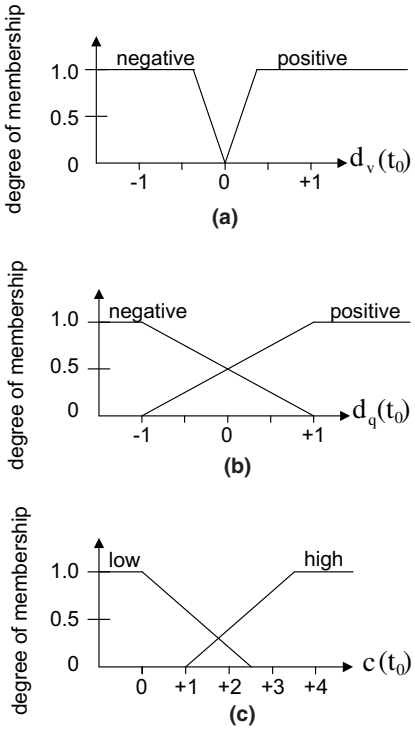


Fig. 16. Fuzzification of the input variables in FOTO with the extended fuzzy logic: (a) $d_v(t_0)$; (b) $d_q(t_0)$; (c) $c(t_0)$.

(6) If the previous (i.e., at the last time interval) traffic phase was not "wide moving jam" and the vehicle speed is "low" and the flow rate is "low" and $d_v(t_0)$ is "negative" and $d_q(t_0)$ is "negative" and $c(t_0)$ is "low", then the traffic phase is "wide moving jam".

(7) If the previous traffic phase was not "wide moving jam" and the vehicle speed is "low" and the flow rate is "low" and $d_v(t_0)$ is "negative" and $d_q(t_0)$ is "negative" and $c(t_0)$ is "high", then the traffic phase is "synchronized flow".

(8) If the previous traffic phase was not "wide moving jam" and the vehicle speed is "low" and the flow rate is "low" and $d_v(t_0)$ is not "negative", then the traffic phase is "synchronized flow".

(9) If the previous traffic phase was not "wide moving jam" and the vehicle speed is "low" and the flow rate is "low" and $d_q(t_0)$ is not "negative", then the traffic phase is "synchronized flow".

(10) If the previous traffic phase was "wide moving jam" and the vehicle speed is "low" and the flow rate is "low" and $d_v(t_0)$ is "positive" and $d_q(t_0)$ is "positive" and $c(t_0)$ is "low", then the traffic phase is "synchronized flow".

(11) If the previous traffic phase was "wide moving jam" and the vehicle speed is "low" and the flow rate is "low" and $d_v(t_0)$ is "positive" and $d_q(t_0)$ is "positive" and $c(t_0)$ is "high", then the traffic phase is "wide moving jam".

(12) If the previous traffic phase was "wide moving jam" and the vehicle speed is "low" and the flow rate is "low" and $d_v(t_0)$ is not "positive", then the traffic phase is "wide moving jam".

(13) If the previous traffic phase was "wide moving jam" and the vehicle speed is "low" and the flow rate is "low" and $d_q(t_0)$ is not "positive", then the traffic phase is "wide moving jam".

## References


Ben-Akiva, M., Koutsopoulos, H., Mukundan, A., 1994. A dynamic traffic model system for ATMS/ATIS operations. IVHS Journal 2 (1).

Cremer, M., 1979. Der Verkehrsfluß auf Schnellstraßen. Springer-Verlag, Berlin.

Daganzo, C., 1994. The cell-transmission model: A dynamic representation of highway traffic consistent with the hydrodynamic theory. Transportation Research B 28, 269–287.

Gartner, N., Messer, C., Rathi, A. (Eds.), 1997. Special Report 165: Revised Monograph on Traffic Flow Theory, Transportation Research Board, Washington, DC.

Helbing, D., 2001. Traffic and related self-driven many particle systems. Reviews of Modern Physics 73, 1067.

Kates, R., Bogenberger, K., 1997. Calibration of the mesoscopic highway simulator ANIMAL: Performance under heavy traffic conditions, 4th World Congress on Intelligent Transport Systems, Berlin.

Kaumann, O., Froese, K., Chrobok, R., Wahle, J., Neubert, L., Schreckenberg, M., 2000. On-line simulation of the freeway network of NRW. In: Helbing, D., Hermann, H.J., Schreckenberg, M., Wolf, D.E. (Eds.), Traffic and Granular Flow '99. Springer, Berlin, pp. 351–356.

Kerner, B.S., 1998a. Experimental features of self-organization in traffic flow. Physical Review Letters 81, 3797–4000.

Kerner, B.S., 1998b. A theory of congested traffic flow. In: Rysgaard, R. (Ed.), Proceedings of the 3rd International Symposium on Freeway Capacity. Road Directorate, Ministry of Transport, Denmark, pp. 621–641.

Kerner, B.S., 1999a. The physics of traffic. Physics World (8), 25–30.

Kerner, B.S., 1999b. Congested traffic flow: Observations and theory. Transportation Research Record 1678, 160–167.

Kerner, B.S., 1999c. Theory of congested traffic flow: Self-organization without bottlenecks. In: Ceder, A. (Ed.), Proceedings of 14th International Symposium of Transportation and Traffic Theory. Elsevier Science Ltd., Oxford, pp. 147–171.

Kerner, B.S., 2000a. Experimental features of the emergence of moving jams in free traffic flow. Journal of Physics A: Mathematical and General 33, L221–L228.

Kerner, B.S., 2000b. Theory of breakdown phenomenon at freeway bottlenecks. Transportation Research Record 1710, 136–144.

Kerner, B.S., 2000c. Phase transitions in traffic flow. In: Helbing, D., Hermann, H.J., Schreckenberg, M., Wolf, D.E. (Eds.), Traffic and Granular Flow '99. Springer, Berlin, pp. 253–284.

Kerner, B.S., 2001a. Complexity of synchronized flow and related problems for basic assumptions of traffic flow theories. Networks and Spatial Economics 1, 35–76.

Kerner, B.S., 2001b. German patent DE 199 44 075 C2, day of notification: 14.09.1999, day of publication: 22.03.2001, patent declaration: 31.01.2002; US patent US 2002045985 (pending); Japan patent JP 2002117481 (pending).

Kerner, B.S., 2002a. Synchronized flow as a new traffic phase and related problems for traffic flow modelling. Mathematical and Computer Modelling 35, 481–508.

Kerner, B.S., 2002b. Empirical macroscopic features of spatial–temporal traffic patterns at highway bottlenecks. Physical Review E 65, 046138.

Kerner, B.S., 2002c. Three-Phase Traffic Theory and Highway Capacity, cond-mat/0211684, e-print in the electronic archive http://arxiv.org/abs/cond-mat/0211684.

Kerner, B.S., 2004a. Three-Phase Traffic Theory and Highway Capacity. Physica A 333, 379–440.

Kerner, B.S., 2004b. The Physics of Traffic. Springer, Berlin, New-York, Tokyo.

Kerner, B.S., Aleksic, M., Denneler, U., 2001. German patent DE 199 44 077 C1, day of notification: 14.09.1999, day of publication: 22.03.2001, patent declaration: 07.02.2002.

Kerner, B.S., Aleksic, M., Rehborn, H., 2000a. Automatic tracing and forecasting of moving traffic jams using predictable features of congested traffic flow. In: Schnieder, E., Becker, U. (Eds.), Proceedings of 9th IFAC Symposium Control in Transportation Systems, vol. 2. IFAC, pp. 501–506.

Kerner, B.S., Aleksic, M., Rehborn, Haug, A., 2000b. A method for the tracing and prediction of traffic flow patterns in the congested regime, In: Proceedings of 7th ITS World Congress on Intelligent Transport Systems, Turin.

Kerner, B.S., Kirschfink, H., Rehborn, H., 1998. German patent DE 196 47 127 C1, day of notification: 14.11.1996, day of publication: 28.05.1998, German patent declaration: 20.04.2000. US-Patent US 5861820. Dutch Patent 100 75 21.

Kerner, B.S., Rehborn, H., 1996a. Experimental properties of complexity in traffic flow. Physical Review E 53, R4257–R4260.

Kerner, B.S., Rehborn, H., 1996b. Experimental features and characteristics of traffic jams. Physical Review E 53, R1297–R1300.

Kerner, B.S., Rehborn, H., 2000. German patent publication DE 198 35 979 A1, day of notification: 08.08.1998, day of publication: 10.02.2000.

Kerner, B.S., Rehborn, H., Aleksic, A., Haug, A., Lange, R., 2000c. Verfolgung und Vorhersage von Verkehrsstörungen auf Autobahnen mit "ASDA" und "FOTO" im online-Betrieb in der Verkehrsrechnerzentrale Rüsselsheim. Straßenverkehrstechnik 10, 521–527.

Kerner, B.S., Rehborn, H., Aleksic, A., Haug, 2001b. Methods for tracing and forecasting of congested traffic patterns on freeways. Traffic Engineering and Control 42 (8), 282–287.

Kerner, B.S., Rehborn, H., Aleksic, A., Haug, A., Lange, R., 2001c. Online automatic tracing and forecasting of traffic patterns. Traffic Engineering and Control 42 (10), 345–350.

Kniss, H.C., 2000. Bewertung des online-Betriebs von ASDA/FOTO in der VRZ Rüsselsheim, (in German), e-print: http://asda-foto.k2s.de.

Koshi, M., Iwasaki, M., Ohkura, I., 1983. Some findings and an overview on vehicular flow characteristics. In: Hurdle, V.F., Hauer, E., Stewart, G.N. (Eds.), Proceedings of 8th International Symposium on Transportation and Traffic Theory. University of Toronto Press, Toronto, Ontario, pp. 403–426.

Kronjäger, W., Konhäuser, P., 1997. Applied traffic flow simulation. In: Papageorgiou, M., Pouliezos, A. (Eds.), Transportation Systems. IFAC, Kreta (Greece), pp. 805–808.

Leutzbach, W., 1988. Introduction to the Theory of Traffic Flow. Springer, Berlin.

May, A.D., Keller, H.M., 1968. Evaluation of single- and two-regime traffic flow models. In: Proceedings of the 3rd International Symposium on Transportation and Traffic Theory. Karlsruhe, Germany, pp. 37–47.

Papageorgiou, M., 1983. Application of Automatic Control Concepts in Traffic Flow Modelling and Control. Springer, Berlin, New York.

Treiterer, J., 1975. Ohio State University Technical Report No. PB 246 094, Columbus, Ohio (unpublished).

Wiedemann, R., 1974. Simulation des Verkehrsflusses, Schriftenreihe des Instituts für Verkehrswesen, Heft 8, Universität (TU) Karlsruhe.